Energy Equip. Sys./ Vol. 5/No1/March 2017/ 43-58

ENERGY EQUIPSYS

Energy Equipment and Systems

http://energyequipsys.ut.ac.ir
www.energyequipsys.com

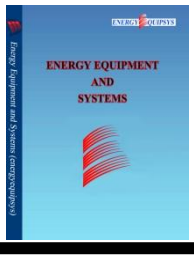

Novel design and simulation of predictive power controller for a doubly-fed induction generator using rotor current in a micro-hydropower plant

Authors

Hamed Javaheri Fard [a]
Hamid Reza Najafi [a*]
Hossein Eliasi [a]

[a] Faculty of Electrical and Computer Engineering, University of Birjand, Birjand, Iran

ABSTRACT

Hydropower plant and especially micro-hydropower plant is an available, reliable and economical energy source. Micro-hydropower plant is one of the most environment-friendly technology, use and development of which leads to reduction of energy consumption sporadically and worldwide. Along with the growth of these power plants, the issues related to the control of electrical parameters such as load, frequency, voltage and power are also constantly rising. This paper describes the proposed structure of variable speed micro-hydropower plant based on Doubly-Fed Induction Generator. The aim is to control the active and reactive powers for this generator. Here, the proposed controller applied to the generator is predictive power controller that adheres to the principle of predictive strategy. Therefore, in this research, a predictive power controller has been proposed to control active and reactive powers of a DFIG based micro-hydropower plant. The control law is acquired by optimizing a cost function considering the tracking factors. The prediction has been performed on basis of a DFIG model. Finally, the stimulations are carried out by Matlab/Simulink to verify the desired performance of controller.

Article history:

Received : 16 September 2016
Accepted : 7 January 2017

Keywords: Rotor Current, Permanent Magnet Synchronous Machine (PMSM), Doubly Fed Induction Generator (DFIG), Predictive Power Controller, Micro-Hydropower Plant.

1. Introduction

Nowadays, energy is the foundation of economic and social progress for each community. The harmful effects of the use of fossil fuels have occupied the minds of scientists and experts for many years. Greenhouse effect, global warming, climate change, increased air pollution are phenomena caused mainly due to the use of fossil fuels.

The use of alternative fuels has always been discussed in international assemblies. Today, renewable energies have achieved a high popularity. Many countries are planning to replace fossil fuels with clean energies that are cheap, environment-friendly and most importantly endless.

Hydro power has long been recognized as a renewable power source [1]. Hydro power plants convert potential energy of water into electricity. It is a clean source of energy [2]. The water after generating electrical power is available for irrigation and other purposes [2].

Micro-hydropower plants are emerging as a major renewable energy resource today as they do not encounter the problems of population displacement and environmental

*Corresponding author: Hamid Reza Najafi
Address: Faculty of Electrical Engineering and Computer, University of Birjand, Birjand, Iran
E-mail address: h.r.najafi@birjand.ac.ir

problems associated with the large hydro power plants [3]. Micro-hydropower plant is a hydroelectric power station which normally produces electrical power up to 100 kW using the natural flow of water.

Topics related to the control of renewable energy conversion systems are constantly growing; and hydroelectric power stations, particularly micro-hydropower plants are not exceptions in this regard. Various studies are published in the scientific literature about the problem of modelling and control of micro-hydropower plants [4-6]. A micro-hydropower plant is usually built in mountains to provide the electricity in rural societies; however, they are mostly isolated and separated from the national power grids. Therefore, they are required to have effective control systems to ensure the sustainability of parameters such as frequency, voltage and power output. Various studies have been conducted in this field. For instance, in [7], the whole set of micro-hydropower plant with electrical machines are available in a model controlled by the fuzzy nonlinear systems. Although the fuzzy technique guarantees stability, it should be noted that the nonlinear constraint may lead to complicated calculations. In [8], the voltage control of the cage rotor induction generator in the micro-hydropower system has been studied in which it is observed that use of this type of generator is not suitable for heavy loads. In [9], control of voltage and frequency of the induction generator has been investigated which is isolated in the micro-hydropower system. The control structure consists of a voltage source inverter along with the dump load circuit at the DC side. In [10], power control of the doubly fed induction generator (DFIG) based on micro-hydroelectric energy conversion system is carried out with the traditional direct power control. Also, the sensorless vector control technique is used to control a permanent magnet synchronous generator in [11]; the sensorless strategies are becoming increasingly popular.

Stability is guaranteed in all these control techniques mentioned above; but efficiency and robustness of these methods are major challenges in order to achieve fast dynamic response, taking into account the uncertainties involved in these power plants and nonlinear case studies.

In this paper, a predictive power controller has been designed and simulated, inspired by a model based on predictive control strategy.

The use of the mentioned strategy covers disadvantages of classical and linear methods such as PID control because the micro-hydropower plant is a non-linear system.

Nomenclature

DFIG	Doubly fed induction generator
PMSM	Permanent magnet synchronous machine
T_T	Turbine torque
Ω	Speed
Ω_e	Rotational speed
dq	Direct axis & Quadrature-axis
MBPC	Model-based predictive control
Ω_n	Nominal speed turbine
P_M	Mechanical power
P_H	Hydraulic power
ρ	Density of water
g	Gravitational acceleration
H	Water level
q	Water rate of flow
T_{PMSM}	PMSG torque
T_{DFIG}	DFIG torque
j	Inertia
ω_{PMSM}	PMSM voltage and current fluctuations
R_{PMSM}	PMSM resistance
$I_{d_{\text{PMSM}}}$	PMSM stator current in the reference d
$I_{q_{\text{PMSM}}}$	PMSM stator current in the reference q
L_d	PMSM inductance in the d reference
L_q	PMSM inductance in the q reference
ϕ_m	Magnetic flux
Np	Number of pairs of poles
R_1	DFIG stator resistance
R_2	DFIG rotor resistance
L_1	DFIG stator inductance
L_2	DFIG rotor inductance
L_M	DFIG mutual inductance
ω_1	DFIG synchronous speed

ω_{mec}	DFIG speed
$\vec{v}$	DFIG voltage vector
P	DFIG active power
Q	DFIG reactive power
$\alpha\beta_r$	Rotor reference frame
δ_s	Position of flux
ω_{sl}	Slip frequency
$\delta_s - \delta_r$	Angle in rotor reference frame
λ	Flux
n_y	Predictive horizon
n_u	Control horizon
tra	Transpose
CF	Cost function
O	Outputs
$f \in \mathrm{R}^{(n_y \times O)\times 1}$	Vector of future output references
$W_y \in \mathrm{R}^{(n_y \times O)\times(n_y \times O)}$	Abbreviation of a defined positive matrix
$W_u \in \mathrm{R}^{n_u \times n_u}$	Abbreviation of a defined positive matrix
$\mathrm{u} \in \mathrm{R}^{n_u \times n_u}$	Input
PF	Power factor
T	Sample time

2. Model Based Predictive Control Strategy

Model based predictive control (MBPC) has played a common and significant role in the novel control engineering in the recent decades. This type of control contains the extensive range of applications in big industries including food industry. The phrase, MBPC, does not represent a particular control procedure; it refers to the wide range of the control methods in which it is possible to obtain a control signal by using minimum of cost function through an explicit processing model [12]. These design methods provide the linear controllers which have similar structures and identical degrees of freedom [12]. The basic idea of the predictive control family is based on the following cases [12]:

- Applying a model to predict the output of the plant in the future.
- Calculating a series control with the aid of minimization of a cost function.
- Applying the receding horizon principle which contains the usage of the first control component in the calculated series control at any moment.

Variant algorithms of predictive control strategy differ among themselves merely in the model used to show the plant, jamming, and the cost function that must be minimized. This control strategy is frequently applied in the industry. Among the applications of this type of control is their usage in robot arm, steam generators, and so on. These applications indicate the capacity of predictive control strategy to achieve the most effective control systems.

In the following, some advantages of MBPC are presented:

- This control strategy can be used to control unlimited fields of processes with simple dynamics or with complicated dynamics; such as the systems with big time delays, the phase non-minimum systems, or the unstable systems [12].
- The multi-variable systems will be easily controlled by this strategy [12].
- This strategy is appropriate for the dead-time systems [12].

3. Micro-hydropower plant

The proposed structure of the micro-hydropower system is shown in Fig.1. These power plants generally are placed in the category of run of river plants, without the need of a water tank such as large dams [13]. Only a small portion of the river's flow is diverted to the turbine. This leads to a useful compromise between the power plants and the environment. In a relevant design, the Kaplan turbine-type impeller is used. The turbine is a reaction turbine with inward flow that takes advantage from axial and radial concepts.

Micro-hydropower is based on a fixed speed synchronous machine and/or a squirrel cage induction generator. In the first case, the speed should be constant; in the second case, speed may vary within a small range regarding the demand in changes of active power or additional capacitance and changes of equivalent load impedance. It is just when the induction machine supply a passive grid, i.e. the power plant is in the islanded state. For both of generators, the rate of turbine flow allows the necessary active power, and frequency control is provided when the power plant is connected to isolated loads. The turbine is connected to a gearbox due to its low rotational speed. This turbine is launched with a DFIG. Excitation of DFIG is performed by a Permanent Magnet Synchronous Machine (PMSM) on the rotor

side of generator. The machine is mounted on the same mechanical shaft. A complete description is presented in relation to the performance and operation of this machine in [14, 15] and for the DFIG in [16, 17]. There are two back to back PWM power electronic converters and the two machines are connected electrically by these converters. A capacitive link is created by the capacitance '*c* ' between the two converters. Stator-side converter of PMSM controls the voltage of capacitive link and the rotor-side converter of DFIG controls this machine in isolated loads or electrical grid [18].

It should be noted that this structure which is based on doubly fed induction generator is different from structures that wind generators use in energy conversion system and the rotor via which the converter is connected to the grid. More information is given about the classical structures of micro-hydropower energy conversion system in [19].

4. Modelling of Micro-Hydropower Plant

In this section, the model of each component of the system is presented so that there is no interaction between system elements.

4.1. Modelling of Impeller Turbine

For the mentioned turbine, a simple model is considered so that the control of both the adjustable blades will not be considered here within the scope of upstream and control of pitch angle blades. Per these assumptions, it is possible to present the behaviour of hydroelectric turbines by static mechanical properties taking a constant flow of rate into account (Fig.2).

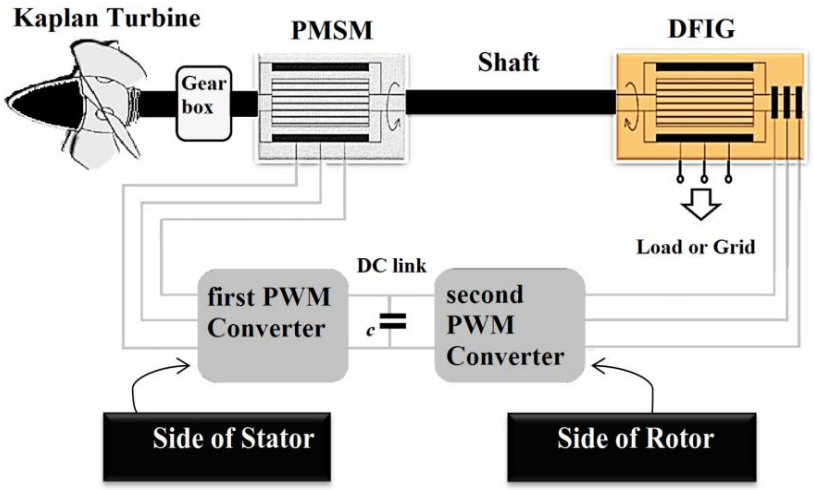

Fig.1. Proposed structure of variable speed micro-hydropower plant

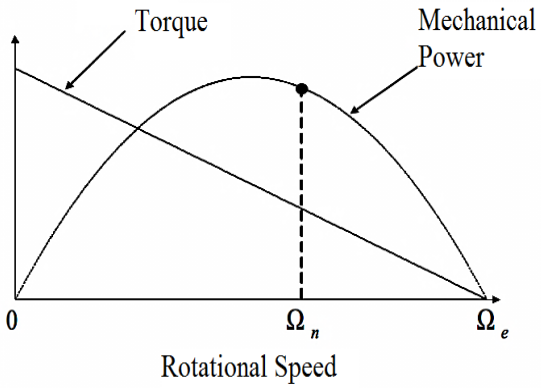

Fig.2. Static mechanical characteristic of hydraulic turbine in a specific flow rate of water

Turbine torque (T_T) versus characteristic of speed (Ω) is assumed to be a straight line. The torque for the rotational speed (Ω_e) is zero; this speed is called runaway. Indeed, this speed will become visible if the load torque is not applied to the shaft [20].

The parameter value (Ω_e) of turbine is assumed 1.8 times of that of nominal speed turbine (Ω_n) [20]. The equation of torque versus speed characteristic equation, under the rate of water flow and with respect to [20] is given in the following,

$$T_T = \{1.8 - (\Omega / \Omega_n)\} T_n \quad (1)$$

The subtitle 'n' represents the nominal value. Simplified characteristic of mechanical power (P_M) is in the form of a parabola. This power can be extracted from the hydraulic power (P_H) which is described below,

$$P_H = \rho \cdot g \cdot H \cdot q \quad (2)$$

In Eq.(2), ρ, g, H, and q are the density of water, gravitational acceleration, water level and flow rate of water, respectively.

4.2. Modelling of the Mechanical Shaft

Derivative of speed in the related electromechanical drive will lead to the production of the applied torques by the turbine and electrical machines on the shaft that corresponds to the following basic equation,

$$\frac{d\Omega}{dt} = \frac{1}{j}(T_T - T_{PMSM} - T_{DFIG}) \quad (3)$$

In Eq.(3), T_{PMSM}, T_{DFIG}, and j are the PMSG torque, DFIG torque and constant inertia in all the rotating parts, respectively.

4.3.Modelling of Permanent Magnet Synchronous Machine (PMSM)

The synchronous machine has been modelled using a park transformation in a reference frame associated with its rotating field. The PMSM stator voltage components in the park are as follows,

$$V_{d_{\mathrm{PMSM}}} = R_{\mathrm{PMSM}} I_{d_{\mathrm{PMSM}}} + L_d \frac{dI_{d_{\mathrm{PMSM}}}}{dt} - \omega_{\mathrm{PMSM}} L_q I_{q_{\mathrm{PMSM}}} \quad (4)$$

$$V_{q_{\mathrm{PMSM}}} = R_{\mathrm{PMSM}} I_{q_{\mathrm{PMSM}}} + L_q \frac{dI_{q_{\mathrm{PMSM}}}}{dt} + \omega_{\mathrm{PMSM}} (L_d I_{d_{\mathrm{PMSM}}} + \phi_m) \quad (5)$$

In fact, the voltages have been separated in form of two components, namely the direct axis d and the orthogonal axis q. In Eqs. (4) and (5), $I_{d_{MSM}} - I_{q_{MSM}}$ and $\omega_{p_{MSM}}$ are stator current in the reference d, stator current in the reference q, voltage and current fluctuations, respectively. Also, R_{PMSM}, L_d, L_q and Φ_m are single phase resistance and single phase inductance in the reference d, single phase inductance in the reference q and magnetic flux produced by the rotor magnets, respectively. The torque generated by the PMSM is expressed as follows,

$$T_{\mathrm{PMSM}} = \frac{3}{2} \mathrm{Np} \{\phi_m I_{q_{\mathrm{PMSM}}} + (L_d - L_q) I_{d_{\mathrm{PMSM}}} I_{q_{\mathrm{PMSM}}}\} \quad (6)$$

where, 'Np' is the number of pairs of poles of the machine. This torque operates in front of the turbine motion when the speed is in the sub-synchronous mode. It will drive up the DFIG in the super synchronous mode; this means that PMSM could operate as a generator or a motor according to the speed of rotation.

4.4.Doubly Fed Induction Generator (DFIG)

The doubly-fed induction generators (DFIG) are equipped with power electronic devices, since they are commonly used for the variable speed turbines [21].

4.4.1. Generator Model and Vector Control of Rotor Current

DFIG model in dq synchronous reference frame is given [22],

$$\vec{v}_{1dq} = R_1 \vec{i}_{1dq} + \frac{d\vec{\lambda}_{1dq}}{dt} + j\omega_1 \vec{\lambda}_{1dq} \quad (7)$$

$$\vec{v}_{2dq} = R_2 \vec{i}_{2dq} + \frac{d\vec{\lambda}_{2dq}}{dt} + j(\omega_1 - \mathrm{NP}\omega_{\mathrm{mec}}) \vec{\lambda}_{2dq} \quad (8)$$

where the relationship between fluxes and currents are as follows,

$$\vec{\lambda}_{1dq} = L_1 \vec{i}_{1dq} + L_M \vec{i}_{2dq} \quad (9)$$

$$\vec{\lambda}_{2dq} = L_M \vec{i}_{1dq} + L_2 \vec{i}_{2dq} \quad (10)$$

Also, active and reactive powers of generator are as follows,

$$P = (3/2)\left[v_{1d} i_{1d} + v_{1q} i_{1q}\right] \quad (11)$$

$$Q = (3/2)\left[v_{1q} i_{1d} - v_{1d} i_{1q}\right] \quad (12)$$

In the above relations, subtitles 1 and 2 show the parameters of the stator and rotor, respectively. $\omega_1, \omega_{mec}, R_1, R_2, L_1, L_2$ and L_M, are the synchronous speed, the speed machine, the electrical resistance of stator and rotor windings per phase, self and mutual inductances of the stator and the rotor windings, respectively. Also, $\vec{v}$ represents the voltage vector and 'NP' indicates the number of pole pairs of generator.

DFIG power control is used for independent control of active and reactive power of stator by adjusting the current rotor. To this end, P and Q are provided as a function of each individual current rotor. We will use the control of the orientation of the stator flux which separates the dq axis; expressed as $\lambda_{1d} = \lambda_1 = \left|\vec{\lambda}_{1dq}\right|$. Therefore, (9) turns to

$$i_{1d} = \frac{\lambda_1}{L_1} - \frac{L_M}{L_1} i_{2d} \quad (13)$$

$$i_{1q} = -\frac{L_M}{L_1} i_{2q} \quad (14)$$

Similarly, using the orientation of stator flux the stator voltage is converted to,

$$v_{1q} = v_1 = \left|\vec{v}_{1dq}\right| \qquad v_{1d} = 0$$

Hence, active power (11) and reactive power (12) can be calculated from (13) and (14),

$$P = -(3/2)\left[v_1 \frac{L_M}{L_1} i_{2q}\right] \quad (15)$$

$$Q = (3/2) v_1 \left[\frac{\lambda_1}{L_1} - \frac{L_M}{L_1} i_{2d}\right] \quad (16)$$

Therefore, the rotor currents will be reflected on the current stator and on the stator active and reactive power, respectively. As a result, this principle is used in stator active and reactive power control of DFIG.

4.4.2. Equations of Rotor Side

Control of the rotor currents using the Eqs. (15) and (16) leads to the control of DFIG power. In the synchronous reference frame using the position of the stator flux and using (13) and (14), rotor voltage in (8) turns into,

$$\vec{v}_{2dq} = \left(R_2 + j\,\sigma L_2 \omega_{sl}\right)\vec{i}_{2dq} + \sigma L_2 \frac{d\vec{i}_{2dq}}{dt} + j\,\frac{L_m}{L_1}\omega_{sl}\lambda_1 \quad (17)$$

where,

$$\omega_{sl} = \omega_1 - \mathrm{Np}\,\omega_{\mathrm{mec}}$$

$$\sigma = 1 - L_M^2 / L_1 L_2$$

In the state space, (17) turns into,

$$\begin{bmatrix} \frac{di_{2d}}{dt} \\ \frac{di_{2q}}{dt} \end{bmatrix} = \begin{pmatrix} \frac{-R_2}{\sigma L_2} & \omega_{sl} \\ -\omega_{sl} & \frac{-R_2}{\sigma L_2} \end{pmatrix} \begin{bmatrix} i_{2d} \\ i_{2q} \end{bmatrix} + \begin{pmatrix} \frac{1}{\sigma L_2} & 0 \\ 0 & \frac{1}{\sigma L_2} \end{pmatrix} \begin{bmatrix} v_{2d} \\ v_{2q} \end{bmatrix} + \begin{pmatrix} 1 & 0 \\ 0 & 1 \end{pmatrix} \begin{bmatrix} 0 \\ \frac{-\omega_{sl} L_M}{\sigma L_1 L_2} \lambda_1 \end{bmatrix} \quad (18)$$

Here, the output matrix is the identity matrix. Henceforth, we assume that mechanical time constant is much greater than the electrical time constant. Therefore, the constant ω_{mec} would be an appropriate approximation for a sample time ' T' [23, 24].

Since the synchronous speed ω_1 is constant with grid and $\omega_{sl} = \omega_1 - \mathrm{Np}.\,\omega_{mec}$, the constant ω_{sl} is also an appropriate approximation for a sample time. Equation (18) can be discrete according to the sampling period and sampling time using the zero-order hold (ZOH) with minimal delay [23].

Therefore, we have,

$$\begin{bmatrix} i_{2d}(k+1) \\ i_{2q}(k+1) \end{bmatrix} = \begin{pmatrix} 1 - \frac{R_2 T}{\sigma L_2} & \omega_{sl} T \\ -\omega_{sl} T & 1 - \frac{R_2 T}{\sigma L_2} \end{pmatrix} \begin{bmatrix} i_{2d}(k) \\ i_{2q}(k) \end{bmatrix} + \begin{pmatrix} \frac{T}{\sigma L_2} & 0 \\ 0 & \frac{T}{\sigma L_2} \end{pmatrix} \begin{bmatrix} v_{2d}(k) \\ v_{2q}(k) \end{bmatrix} + \begin{pmatrix} 1 & 0 \\ 0 & 1 \end{pmatrix} \begin{bmatrix} 0 \\ \frac{-\omega_{sl} L_M T}{\sigma L_1 L_2} \lambda_1(k) \end{bmatrix} \quad (19)$$

4.4.3. Model Based Predictive Controller for DFIG Power Control

In this paper, prediction of the output is obtained from the state-space model and has been shown by the following equation,

$$\mathrm{y} = G_{gx} x_k + M\ \mathrm{u} + N\,\omega_k \quad (20)$$

where,

$$\mathrm{y} = \begin{bmatrix} y(k+1) \\ y(k+2) \\ \vdots \\ y(k+n_y) \end{bmatrix} \quad (21)$$

$$\mathrm{u}=\begin{bmatrix} u(k) \\ u(k+1) \\ \vdots \\ u(k+n_y-1) \end{bmatrix} \quad (22)$$

Also, the matrix x_k is $\begin{bmatrix} i_{2d}(k) \\ i_{2q}(k) \end{bmatrix}$ and the matrix ω_k is $\begin{bmatrix} 0 \\ \frac{-\omega_{sl} L_M T}{\sigma L_1 L_2} \lambda_1(k) \end{bmatrix}$. also,

$$G_{gx}=\begin{bmatrix} \mathrm{C'A'} \\ \mathrm{C'A'^2} \\ \mathrm{C'A'^3} \\ \vdots \\ \mathrm{C'A'^{n_y}} \end{bmatrix} \quad (23)$$

and,

$$M=\begin{bmatrix} \mathrm{C'B'} & 0 & 0 & 0 \\ \mathrm{C'A'B'} & \mathrm{C'B'} & 0 & 0 \\ \mathrm{C'A'^2B'} & \mathrm{C'A'B'} & \mathrm{C'B'} & 0 \\ \vdots & \vdots & \vdots & \vdots \\ \mathrm{C'A'^{n_y-1}B'} & \mathrm{C'A'^{n_y-2}B'} & \mathrm{C'A'^{n_y-3}B'} & \ldots \end{bmatrix} \quad (24)$$

and,

$$N=\begin{bmatrix} \mathrm{C'} & 0 & 0 & \ldots & 0 \\ \mathrm{C'A'} & \mathrm{C'} & 0 & \ldots & 0 \\ \mathrm{C'A'^2} & \mathrm{C'A'} & \mathrm{C'} & \ldots & 0 \\ \vdots & \vdots & \vdots & \vdots & \\ \mathrm{C'A'^{n_y-1}} & \mathrm{C'A'^{n_y-2}} & \mathrm{C'A'^{n_y-3}} & \ldots & \mathrm{C'} \end{bmatrix} \quad (25)$$

where,

$$\mathrm{A'}=\begin{pmatrix} 1-\frac{R_2 T}{\sigma L_2} & \omega_{sl} T \\ -\omega_{sl} T & 1-\frac{R_2 T}{\sigma L_2} \end{pmatrix}$$

$$\mathrm{B'}=\begin{pmatrix} 1-\frac{R_2 T}{\sigma L_2} & \omega_{sl} T \\ -\omega_{sl} T & 1-\frac{R_2 T}{\sigma L_2} \end{pmatrix}$$

$$\mathrm{C'}=\begin{pmatrix} 1 & 0 \\ 0 & 1 \end{pmatrix} \quad (26)$$

where, 'n_y' represents the output of prediction horizon. Choosing the prediction horizon 'n_y' for control performance is critical; i.e. selecting a large value for this parameter improves the system stability, but may increase the computational cost significantly. The state variables are estimated by the sensors from the rotor speed, the stator voltages and the measured currents.

The control law is obtained with minimization of a quadratic cost function which also represents the error between the predicted values and the future references. The quadratic function is given as a matrix in the following equation,

$$\mathrm{C.F}=\left\{(\mathrm{y}-f)^{\mathrm{tr}} W_y (\mathrm{y}-f)\right\}+\left\{\mathrm{u}^{\mathrm{tr}} W_u \mathrm{u}\right\} \quad (26)$$

where, $f \in \mathrm{R}^{(n_y \times O \times 1)}$ represents the vector of future output references; $W_y \in \mathrm{R}^{(n_y \times O)\times(n_y \times O)}$ is the abbreviation of a defined positive matrix that is effective on each controlled outputs and its predictions; $W_u \in \mathrm{R}^{n_u \times n_u}$ is abbreviation of a defined positive matrix, usually diameter, which gives weight to the inputs control efforts; $\mathrm{u} \in \mathrm{R}^{n_u \times n_u}$ is the input, ' O is the number of outputs, and n_u is control horizon.

The mode n_u =1 represents which of the input domains have an average value; this means that the output values track the reference values accurately. At the mode n_u >1, control strategy generates control signals which makes the output track the reference more closely. A large amount for n_u produces high control signals and computational costs increase too much. The matrix W_u is reflected in the control effort. Elements of W_u are not zero since these values effect into the controller response with high overshoot when they are null. Therefore, when the elements are equal to zero, the actuator can provide infinite energy and this issue do not correspond in any way with the real devices which have some limitations. It is worth noting that a method for calculating the matrix elements W_y from a nonlinear system is presented in [25]. However, the computational cost involved in this procedure is important. In the cost function (26), the model is linear. The minimum value of the cost function can be determined from $\partial \mathrm{C.F}/\partial \mathrm{u}=0$ algebraically. Since G_{gx}, M and N are interrelated to the estimated states; they should be updated for each control cycle. Results in a quadratic cost function are dependent on 'u' by replacing 'y' from (20) to (26), which also gives the optimal analytical solution.

The control law has been obtained with the help of minimum amount of cost function, by creating $\partial C.F/\partial u = 0$ and separation of 'u'. Thus, this expression is given by (27),

$$u = (M^{tr} W_y M + W_u)^{-1} M^{tr} W_y (f - G_{gx} x_k - N \omega_k) \quad (27)$$

MBPC diagram applied for power control of DFIG is shown in Fig.3.

By using (27), the proposed controller generates rotor voltages that allow the convergence of active and reactive powers with their respective reference values. The desired rotor voltage in the rotor reference frame $\alpha\beta_r$ also produces the switching signals for the side of rotor using space vector modulation method; which is given by,

$$\vec{v}_{2\alpha\beta_r} = \vec{v}_{2dq} (e^{\delta_s - \delta_r})$$

Currents and voltages of stator as well currents and speed of rotor are measured in order to estimate the position of the stator flux δ_s and the amplitude λ_1, synchronous frequency ω_1 and slip frequency ω_{sl}.

The reference rotor current for active power control is derived by using (15),

$$i_{2q_{ref}} = -\frac{2P_{ref} L_1}{3v_1 L_M} \quad (28)$$

The reference rotor current for reactive power control using (16) is as follows,

$$i_{2d_{ref}} = -\frac{2q_{ref} L_1}{3v_1 L_M} + \frac{\lambda_1}{L_M} \quad (29)$$

4.4.4. Estimation of Parameters

In order to calculate the active and reactive powers of the proposed controller, the required components are: presence of the stator amplitude, position of stator flux, sliding speed and the synchronous frequency. The estimation of flux by using (7) will be as follows,

$$\vec{\lambda}_{1\alpha\beta} = \int (\vec{v}_{\alpha\beta} - R_1 \vec{i}_{1\alpha\beta}) dt \quad (30)$$

The position of flux by using (30) will be as follows,

$$\delta_s = \tan^{-1}\left(\frac{\lambda_{1\beta}}{\lambda_{1\alpha}}\right) \quad (31)$$

The estimation of synchronous frequency is given by the following equation,

$$\omega_1 = \frac{d\delta_s}{dt} = \frac{(v_{1\beta} - R_1 i_{1\beta})\lambda_{1\alpha} - (v_{1\alpha} - R_1 i_{1\alpha})\lambda_{1\beta}}{(\lambda_{1\alpha})^2 + (\lambda_{1\beta})^2} \quad (32)$$

Also, estimation of slip frequency by using the rotor speed and synchronous frequency be as follows,

$$\omega_{sl} = \omega_1 - \mathrm{Np}\omega_{mec} \quad (33)$$

and finally, the angle in the rotor reference frame is given by the following equation,

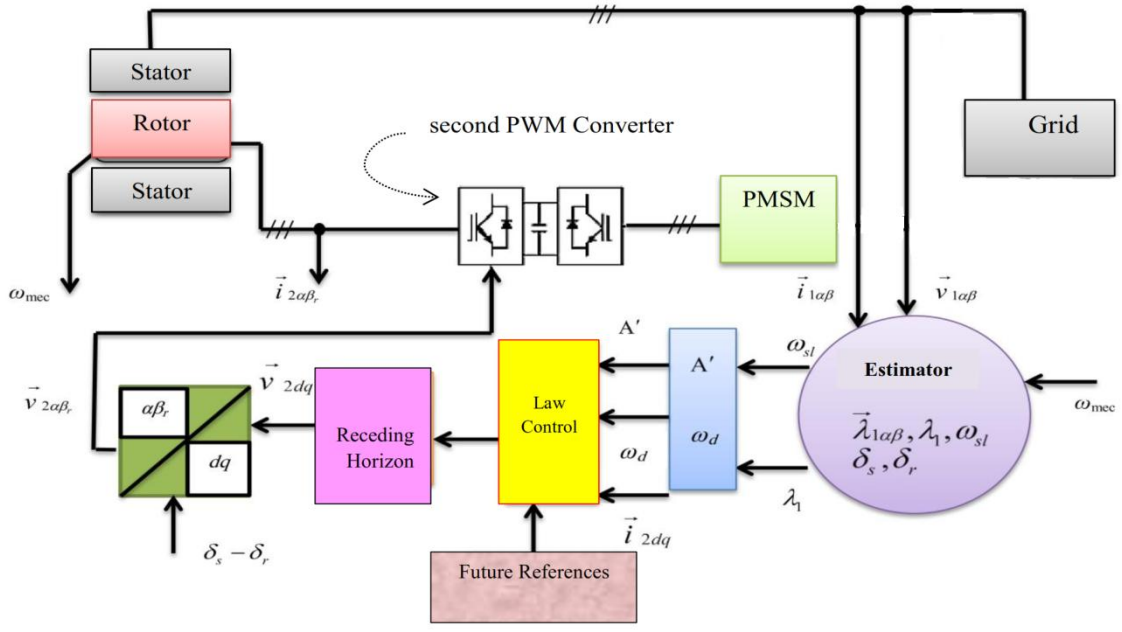

Fig. 3. Block diagram of the proposed predictive controller

$$\delta_s - \delta_r = \int \omega_{sl} dt \quad (34)$$

5. Simulation Results

In this section, simulation tests of the proposed predictive power controller for the doubly-fed induction generator based on micro-hydropower energy conversion system are presented. To begin the simulation, both machine parameters are determined as Table 1.

The three-phase line voltages are 230 V and voltage link capacitor is 150 V. The sampling time of controller is 25 μSec. DFIG and PMSM are Np = 2 and Np = 4, respectively.

Rate of flow of water is constant in the micro-hydropower energy conversion system that is connected to the power grid; this is due to the variability of rate of flow of water which has a time scale of hours to days.

In this section, simulation of desired system is done by the applications Matlab and/or Simulink.

It is worth mentioning that to control the power factor (PF), reference reactive power is given by the following equation,

$$Q_{ref} = P_{ref} \frac{\sqrt{1-\mathrm{PF}^2}}{\mathrm{PF}} \quad (35)$$

Moreover, the weighted elements must be carefully regulated in the matrices W_y and W_u so that they are consistent with favourable conditions of designer. It has been found that the matrix W_u is associated with the control effort and its elements should be non-zero due to the presence of high overshoot. Also, the matrix W_y confirms every unique prediction of output that improves response time of process.

Therefore, with this description, the value of matrices W_y and W_u will be designated as follows,

$$W_y = [10 \quad 0 \quad ; \quad 0 \quad 30]$$

$$W_u = [0.003 \quad 0 \quad ; \quad 0 \quad 0.02]$$

Note that these two matrices are written in the m-file/ Matlab in accordance with above form.

In Fig. 4, the three-phase stator current of DFIG is given. As it can be easily recognized, these currents are quite sine. This major issue is perceptible and visible with the development of simulation time that ranges from 3 to 3.5 Sec.

In the next sections, this issue can be better understood with the frequency analysis.

The rapid response and robust currents can be seen, so this issue is directly related to proposed controller and the detailed design parameters.

In Fig. 5, the three-phase rotor current of DFIG is depicted. Also, similar to the previous case for the rotor currents with complex density, here the simulation times are expanded ranging from 3 to 3.5 Sec. It can be observed that these currents will also be the sine. It should be noted that the current overshoot in the response of three-phase stator and rotor currents is very low.

In order to verify the effectiveness and the impact of predictive controller proposed in this paper, comparative tests have been assigned between the direct power control (classical technique in [10]) and predictive power control strategy proposed herein. Thus, Fig. 6 shows the three-phase stator current DFIG in a micro-hydropower plant, which has been obtained from the DPC technique and [10].

With this comparison, it can be easily understood that DFIG stator current, obtained from the classic technique, has much more ripple than the advanced strategy proposed in this paper. Of course, the currents have been developed in a certain time interval in order to be viewed better and more accurately, as shown in Fig. 6. This comparison can be generalized to the three-phase rotor currents obtained by the two methods. The three-phase rotor currents, obtained through the classic technique [10], can be seen in Fig. 7.

Table.1. Machines parameters

DFIG Parameters		PMSM Parameters	
R_1	1.34 Ω	R_{PMSM}	0.76 Ω
R_2	0.45 Ω	L_d	0.017 H
L_M	0.055 H	L_q	0.033 H
L_1	0.0135 H	j	0.0018 kgm^2
L_2	0.0255 H		
j	0.0017kgm^2		

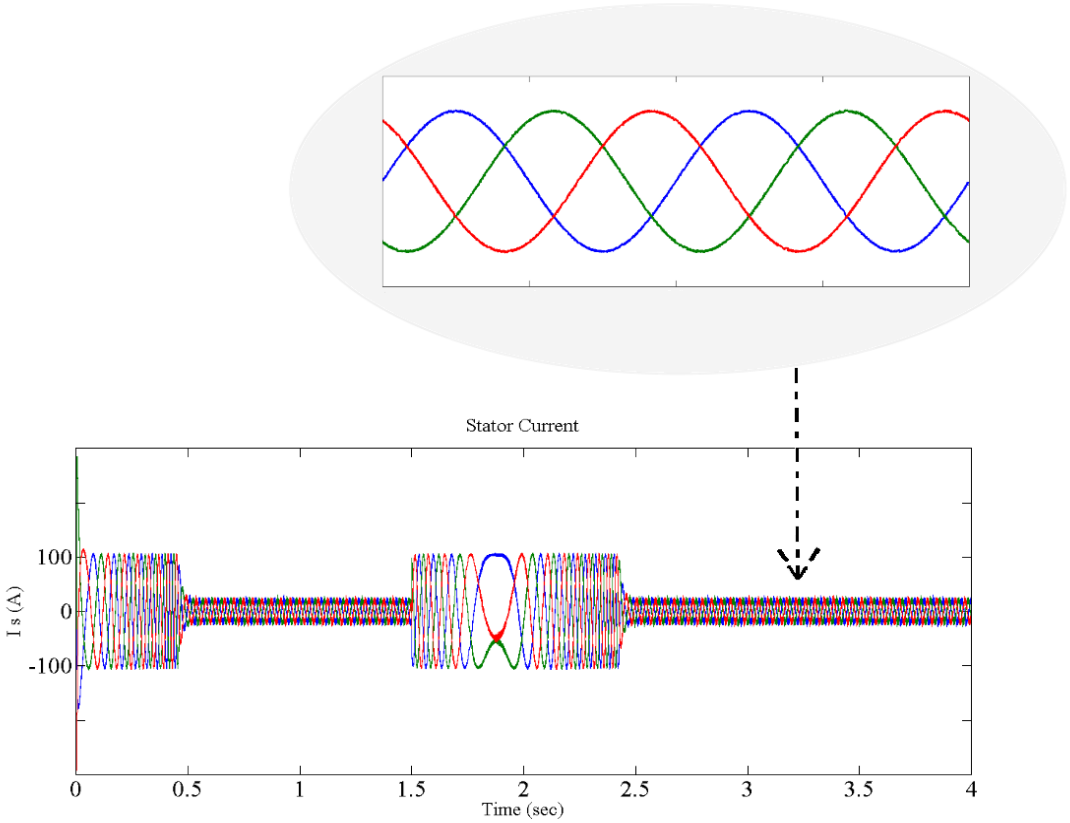

Fig. 4. DFIG stator current

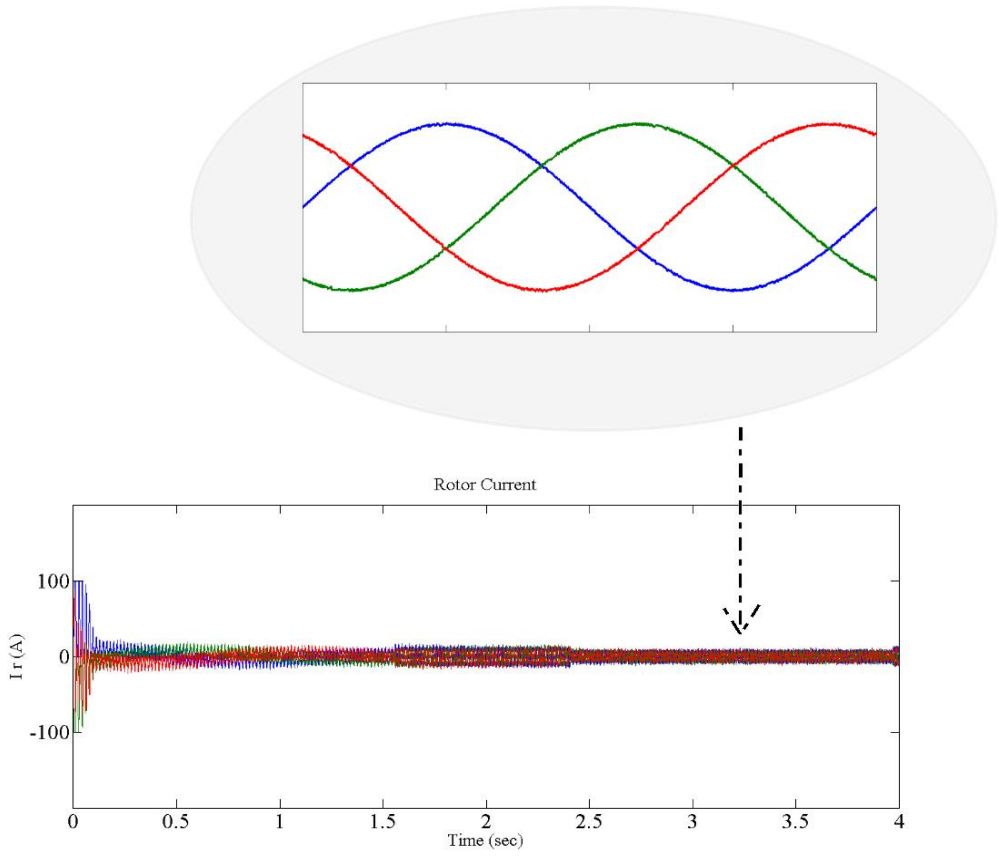

Fig. 5. DFIG rotor current

Again, it is observed that the ripple is indeed more sensible in these currents, compared to the currents seen in Fig. 5. In Fig. 7, currents have been developed in a certain time interval, too.

Therefore, it is evident that the strength of predictive control strategy proposed in this paper is remarkable.

If the frequency spectrum analysis (FFT) is done on one of the phases of the stator and rotor currents, total harmonic distortion (THD) is obtained. It is a qualitative parameter that indicates how close a waveform or signal is to the sinusoidal. The lower value of THD represents the better quality of sinusoidal waveform. Analyses of the frequency spectrum are given in Fig. 8 and Fig. 9, respectively. In Fig. 8, which corresponds to single-phase stator current of DFIG, THD is very low (1.52%). Similarly, it can be seen in Fig. 9 that the single-phase rotor current has even less THD, i.e. 1.46 %.

Studies will be continued with steps of active and reactive powers for testing the dynamic response of the proposed power controller. DFIG reactive power and DFIG active power are depicted in Fig.10 and in Fig. 11, respectively. Reactive power has a value of -750 VAr at the beginning of the simulation period (0 Sec to 1.5 Sec); the power factor so far is 0.85. From 1.5 Sec to 2.4 Sec, the amount of reactive power will be 1400 VAr; the power is reduced from this time point onwards till 3.9 Sec. Thus, it again reaches the initial amount of -750 VAr; finally, from the time 3.9 Sec to the end, reactive power is fixed on zero; and this means that according to $Q = VI \sin \varphi$, power factor is one ($\cos \varphi = 1$). As seen in Fig. 10, in all these moments, reactive powers always follow their own reference value and track them.

It is observed that reactive power has extremely low ripple so it can even be over

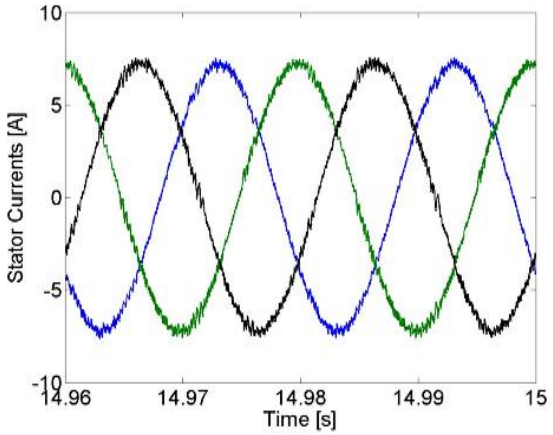

Fig.6. DFIG stator current obtained by DPC technique [10]

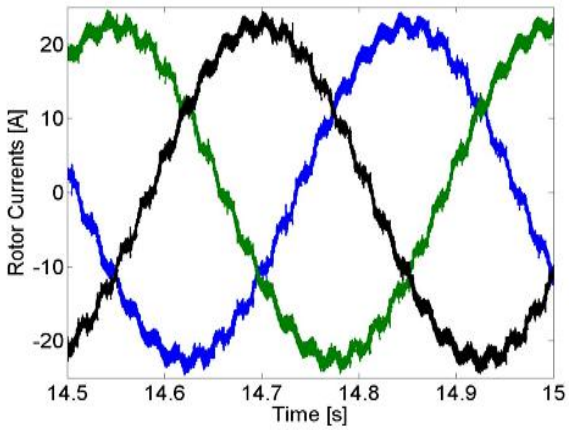

Fig. 7. DFIG rotor current obtained by DPC technique [10]

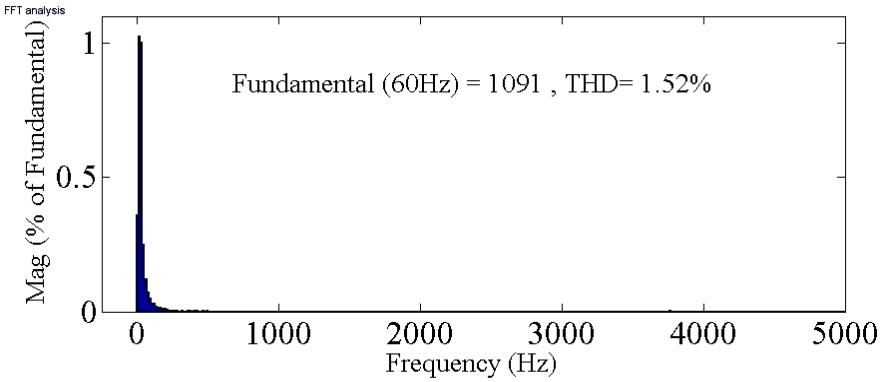

Fig. 8. Stator current frequency spectrum analysis

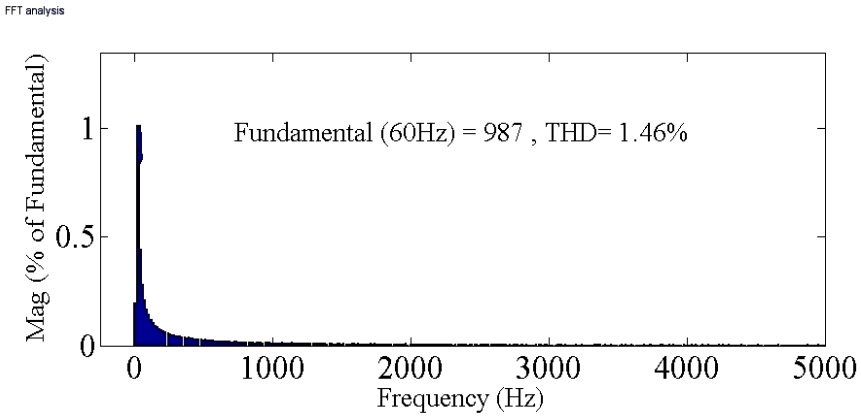

Fig. 9. Rotor current frequency spectrum analysis

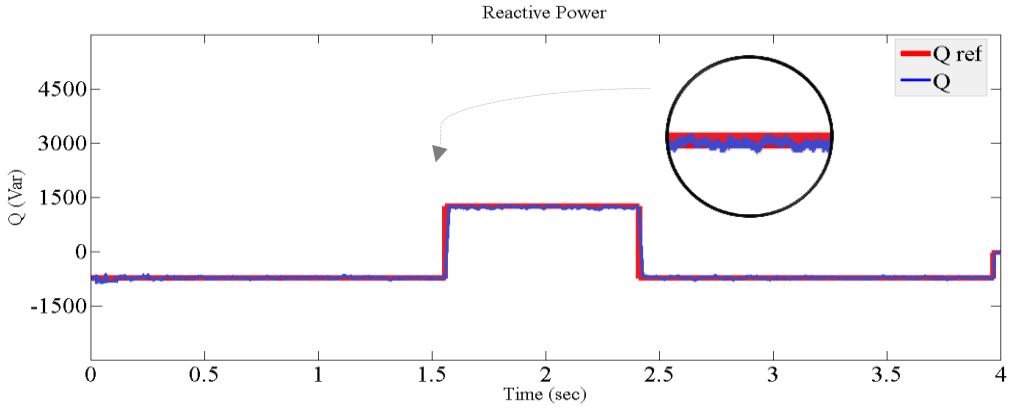

Fig.10. DFIG reactive power with their reference values

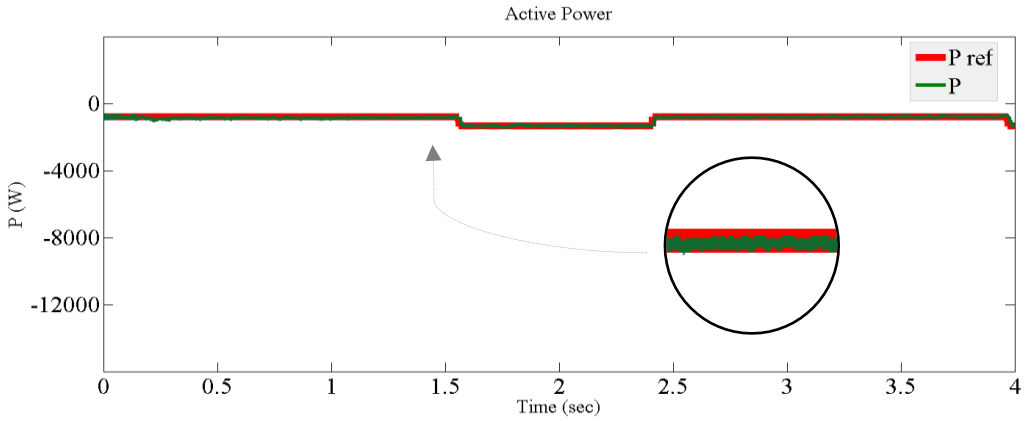

Fig.11. DFIG active power with their reference values

looked. This issue shows robustness and effectiveness of the proposed controller.

All of the tips mentioned above in the case of reactive power, as well as about active power are true. It is observed from Fig. 11 that at the beginning of the simulation, namely at 0 Sec to 1.5 Sec, this power has a value of -1000 W. Active power decreases from 1.5 Sec to 2.4 Sec and it reaches -1500 W; but from this time to 3.9 Sec, active power increases and it reaches to its initial value again. It can be seen in Fig. 13 that active power reaches very low ripple because the controller parameters are well-designed and accurate. It should be noted that the active power tracks the reference values with great accuracy. In fact, it is obvious that there is no overshoot in both powers.

If the active and reactive powers derived from the proposed strategy are compared with the powers gained from the classical technique in [10], superiority of predictive control strategy again becomes clear regarding accurate, robust and efficient

responses. This can be noted from Fig. 12 that the two powers are associated with intensive ripple in the timeframe. Of course, the amplitudes of these fluctuations are acceptable.

In fact, considering Fig. 10 and Fig. 11, we can see that they are not comparable.

DFIG currents of rotor's *q* & *d* components are given in Fig. 13 and Fig. 14, respectively. Both forms had low fluctuations. Both the currents showed a little overshoot in a fraction of a second at the start of simulation. They closely tracked their reference values; this is one of the benefits of the proposed controller.

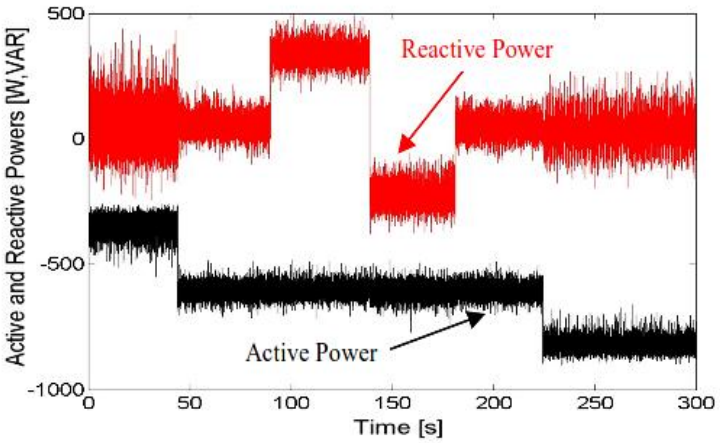

Fig.1. DFIG active and reactive powers obtained by DPC technique [10]

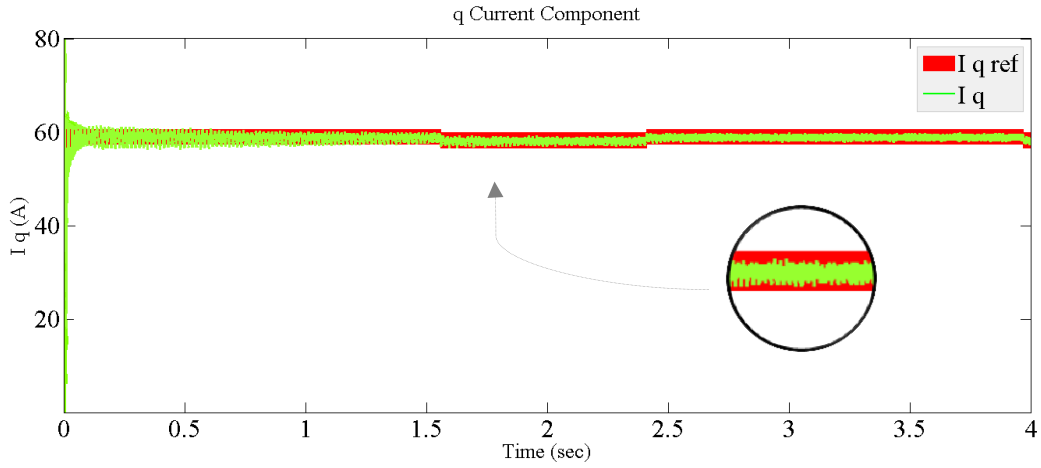

Fig.13. DFIG current of rotor's *q* component with their reference values

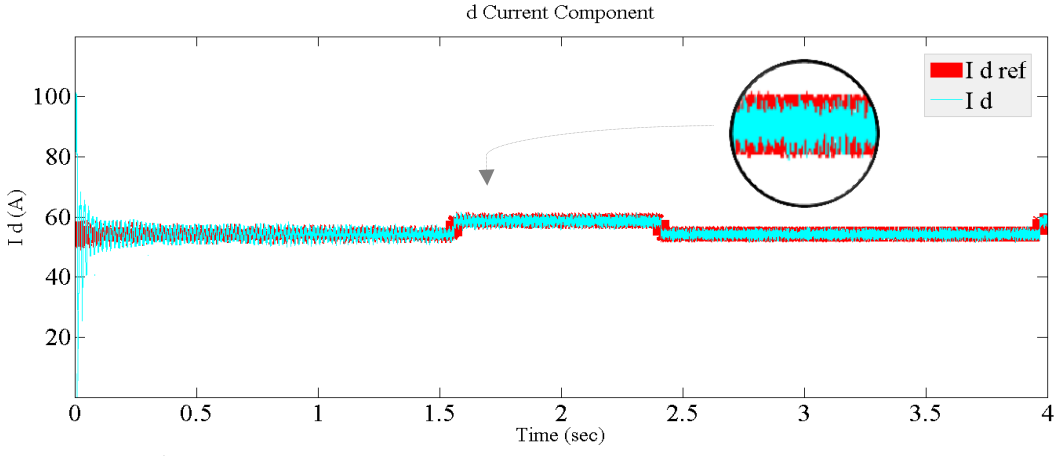

Fig.14. DFIG current of rotor's d component with their reference values

In Fig. 15, a simulated waveform DC-link voltage (capacitor) is depicted. It is evident that the voltage remained constant throughout the simulation time. This voltage shows favourable dynamic performance. This voltage had fully robust and stable behaviour even at transient states; such result is obtained because the parameters of controller are accurately designed.

By comparing the behaviour of capacitive link voltage gained from the proposed strategy with that of the classical technique, it was observed that voltage at DPC presented ripple if the period of simulation was expanded. The capacitive link voltage, obtained from the [10], can be seen in Fig. 16.

At the end of the simulation, mechanical speed from micro-hydropower system is given in Fig. 17 in terms of rpm as a final data. This represents the speed of the system shaft. Note that this speed is related to the active power machine and indicates that DFIG is working properly. In Fig. 17, it can be seen that speed has reacted in intended time smoothly and its path goes to the super synchronous and sub-synchronous ranges of induction machine.

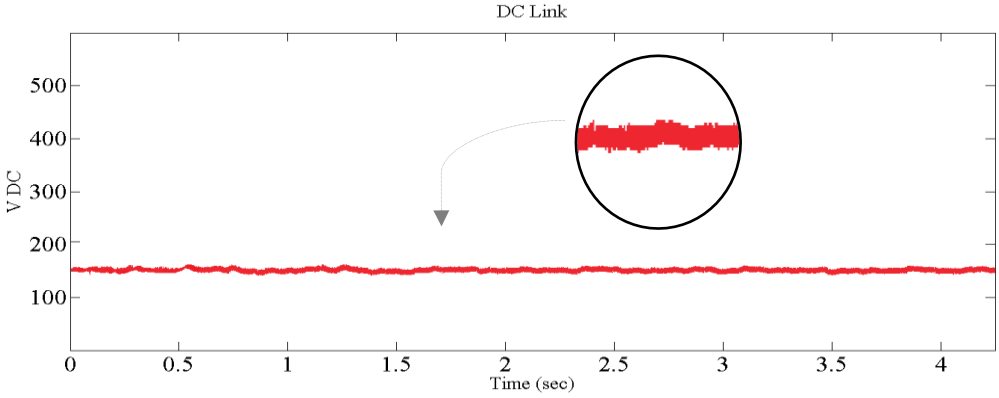

Fig.15. DC-link voltage obtained proposed controller

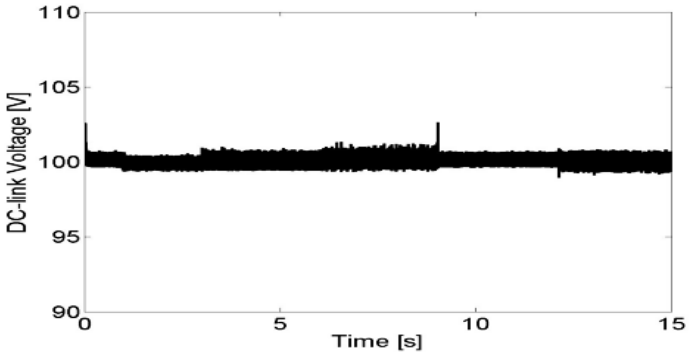

Fig.16. DC-link voltage obtained DPC [10]

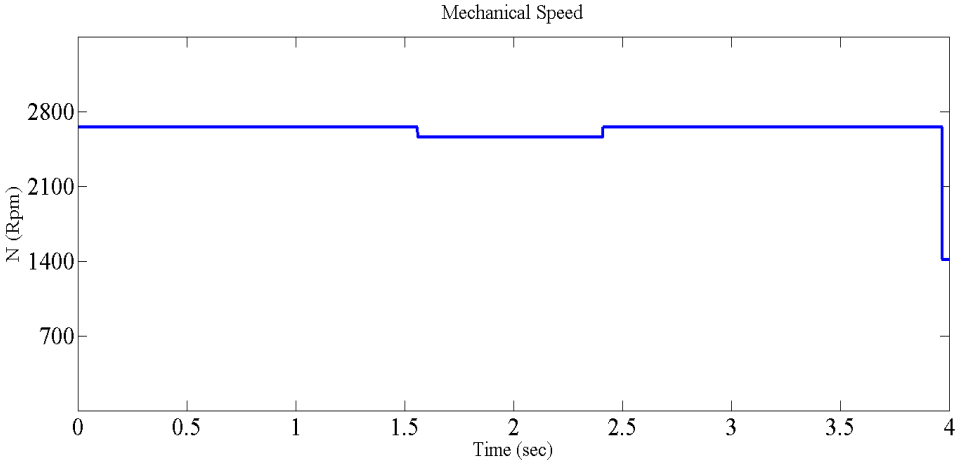

Fig.17. Mechanical speed of micro-hydropower plant obtained from proposed controller

5. Conclusion

In this paper, a model-based predictive controller was designed and simulated for controlling the active and reactive powers of a doubly fed induction generator (DFIG) in the energy industry, based on micro- hydropower plant energy conversion system and using current from the rotor's d & q components. As discussed, predictive controller was based on a model the implementation of which was easy in order to control the DFIG. The predicted outputs had been calculated with the help of a state-space model of DFIG. The control system was composed of a control law that was extracted from optimizing a cost function. The cost function considers control effort and the difference between predicted outputs (active and reactive power) and the reference values. Rotor voltage control was calculated with the receding horizon method, while the states constraints were satisfied. It should be noted that the use of the proposed control strategy provides a constant switching frequency.

In fact, the dynamic response obtained from the simulations demonstrates accuracy of the proposed predictive control strategy. Note that if the design of parameters such as parameters included in cost function is done correctly, the accuracy of the simulations will increase. For example, changing the weighting matrices will definitely affect the system stability or change machine parameters.

Finally, controller was designed and simulated with Matlab/Simulink software. The simulation results specified the robustness and effectiveness of this controller. Also, in order to prove the effectiveness and efficiency of the proposed predictive controller, comparative analysis was carried out between direct power control (classical method is described in [10]) and proposed predictive power control strategy. In the proposed strategy, the results of dynamic responses were quite fast and overshoot on some parameters and non-existent or very low in others. Future research will aim at the implementation of predictive control strategy based on other renewable resources such as tidal energy. This topic will be discussed in future scientific communications. For more information about the predictive control strategy and its applications in the electrical engineering industry, especially power and energy branch, refer to [26-29].

References

[1] Garcia F. J., Uemori M. K. I., Echeverria J. J. R., Da Costa Bortoni E., Design Requirements of Generators Applied to Low-Head Hydro Power Plants, IEEE Transactions on Energy Conversion, (2015) 30(4): 1630 – 1638.

[2] Mohibullah M., Radzi A. M., Hakim M. I. A.,Basic Design Aspects of Micro Hydro Power Plant and Its Potential Development in Malaysia, Power and Energy Conference, IEEE International Conference on Power and Energy Proceedings(2004)220 – 223.

[3] Hanmandlu M., Goyal H., Kothari D. P., An Advanced Control Scheme for Micro Hydro Power Plants, Power Electronics, Drives and Energy Systems, PEDES '06. International Conference on, IEEE (2006)1-7.

[4] Laghari J.A., Mokhlis H., Bakar A.H.A., Hasmaini M., A Comprehensive Overview of New Designs in the Hydraulic, Electrical Equipment and Controllers Of Mini Hydro Power Plants Making It Cost Effective Technology, Renewable and Sustainable Energy Reviews, Elsevier (2013) 279 – 293.

[5] Monteiro C., Ramirez-Rosado I. J., Fernandez-Jimenez L. A.,Short-Term Forecasting Model for Electric Power Production of Small-Hydro Power Plants, Renewable Energy, Elsevier (2013) 50:387 – 394.

[6] Kishor N., Saini R.P., Singh S.P., A Review on Hydropower Plant Models and Control, International Journal of Mechatronics, Electrical and Computer Technology, Elsevier, IEEE (2004)776 – 796.

[7] Salhi I., Doubabi S., Essounbouli N., Hamzaoui A., Application of Multi-Model Control With Fuzzy Switching to a Micro Hydro-Electrical Power Plant, Renewable Energy, Elsevier (2010) 35: 2071 – 2079.

[8] Wang G., Zhai Q., Yang J.,Voltage Control of Cage Induction Generator in Micro Hydro Based on Variable Excitation, Electrical Machines and Systems (ICEMS), International Conference on, IEEE (2011) 13(4): 1-3.

[9] Ion C.P., Marinescu C.,Autonomous Micro Hydro Power Plant with Induction Generator, Renewable Energy, Elsevier (2011) 36: 2259 – 2267.

[10] Breban S., Radulescu M. M., Robyns B., Direct Active and Reactive Power Control of Variable-Speed Doubly-Fed Induction Generator on Micro-Hydro Energy Conversion System, Xix International

Conference on Electrical Machines - ICEM, Rome, IEEE (2010)1-6.
[11] Löhdefink P., Grillenberger M., Dietz A., Gröger A., Hoffmann A., Hubert T., Sensorless Vector Control of a Permanent Magnet Synchronous Generator for Micro Hydro Power, Education and Research Conference (EDERC), IEEE, 5th European DSP (2012) 252 - 256.
[12] Camacho E., Bordons A.C., Model Predictive Control, Springer, Book (2004).
[13] Molina M.G., Pacas M., Improved Power Conditioning System of Micro-Hydro Power Plant For Distributed Generation Applications, Industrial Technology (ICIT), IEEE International Conference on (2010)1733 - 1738.
[14] Jahns T.M., Variable Frequency Permanent Magnet AC Machine Drives, Wiley, Book (2013).
[15] M.A.C, Martinez-Botas R.F., Lamperth M., Measurement of Magnet Losses in a Surface Mounted Permanent Magnet Synchronous Machine, Energy Conversion, IEEE Transactions (2015) 30: 323-330.
[16] Wu B., Lang Y., Zargari N., Kouro S., Doubly Fed Induction Generator Based Wecs, Wiley, Book (2011).
[17] Variani M.H., Tomsovic K., Two-Level Control of Doubly Fed Induction Generator Using Flatness-Based Approach, IEEE Transactions, Power Systems (2015)1-8.
[18] Breban S., Nasser M., Ansel A., Saudemont C., Robyns B., Radulescu M., Variable Speed Small Hydro Power Plant Connected to Ac Grid or Isolated Loads, EPE Journal (2007)17: 29 - 36.
[19] Ansel A., Biet M., Robyns B., Micro Hydropower Station Based on a Doubly Fed Induction Generator Excited by a Pm Synchronous Machine, ICEM (2004).
[20] Petites Centrales Hydrauliques-Turbines Hydrauliques, Report of the Renewable Energies Action Program in Switzerland, PACER (1995).
[21] Miryousefi Aval S. M., Ahadi A.,Wind Turbine Fault Diagnosis Techniques and Related Algorithms, International Journal of Renewable Energy Research-IJRER (2016)6: 80-89.
[22] Leonhard W.,Control of Electrical Drives. Berlin, Germany, Springer (1985).
[23] Filho A. J. S., Ruppert E., A Deadbeat Active and Reactive Power Control for Doubly – Fed Induction Generator, Electric Power Components and Systems (2010) 38: 592 – 602.
[23] Filho A. J. S., Filho E. R., The Complex Controller for Three-Phase Induction Motor Direct Torque Control, Controle & Automação Sociedade Brasileira de Automatica (2009) 20:256-262.
[24] An A., Hao X., Zhao C., Su H., A Pragmatic Approach for Selecting Weight Matrix Coefficients in Model Predictive Control Algorithm and Its Application, In proceedings IEEE International Conference on Automation and Logistics (2009) 486-492.
[25] Javaheri Fard H., Najafi H.R., Eliasi H., Active and Reactive Power Control Via Currents of Rotor's d and q Components with Nonlinear Predictive Control Strategy in Doubly-Fed Induction Generator Based on Wind Power System, Energy Equipment and Systems (2015)3:143-157.
[26] Javaheri Fard H., Najafi H.R., Heidari G., Design of Discrete Predictive Direct Power Control Strategy on the Doubly-Fed Induction Generator Based on Micro-Hydro Power Plant With the Aim of Active and Reactive Powers Control, 21st Conference on Electrical Power Distribution Networks Conference (Epdc) IEEE (2016) 118-124.
[27] Javaheri Fard H., Najafi H.R., Eliasi H., Design and Implementation of the Predictive Current Control Strategy in the Form of Laboratory on Single Phase Photovoltaic Grid-Connected Inverter Based on Microcontroller Tms320lf2407a, 30 th International Power System Conference (PSC) (2015) 1-7.
[29] Eliasi H., Menhaj M.B., Davilu H., Robust Nonlinear Model Predictive Control for a PWR Nuclear Power Plant, Progress in Nuclear Energy, Elsevier, (2012) 54: 177-185.